1 **Street RABV induces the cholinergic anti-inflammatory pathway in human monocyte-**

2 **derived macrophages by binding to nAChr α7, and upregulates the M2-c marker CD163**

3

4 **Short title:**

5 **Street RABV induces anti-inflammatory pathways in human macrophages**

6

7

8 C.W.E. Embregts[1], L. Begeman[1], C.J. Voesenek[2], B.E.E. Martina[1], M.P.G. Koopmans[1], T.

9 Kuiken[1], C.H. GeurtsvanKessel[1]

10

11 **Affiliations**

12 [1] Department of Viroscience, Erasmus Medical Center, Rotterdam, the Netherlands

13 [2] Independent researcher

1

14   **Abstract**

15

16   Rabies virus (RABV) is able to reach the central nervous system (CNS) without triggering a strong

17   immune response, using multiple mechanisms to evade and suppress the host immune system.

18   After infection via a bite or scratch from a rabid animal, RABV comes into contact with

19   macrophages, which are the first antigen-presenting cells (APCs) that are recruited to the area and

20   play an essential role in the onset of a specific immune response. It is poorly understood how

21   RABV affects macrophages, and if the interaction contributes to the observed immune

22   suppression. This study was undertaken to characterize the interactions between RABV and human

23   monocyte-derived macrophages (MDMs). We showed that street RABV does not replicate in

24   human MDMs. Using a recombinant trimeric RABV glycoprotein (RABV-tG) we showed binding

25   to the nicotinic acetylcholine receptor alpha 7 (nAChr α7) on MDMs, and confirmed the specificity

26   using the nAChr α7 antagonist alpha-bungarotoxin (α-BTX). We found that this binding induced

27   the cholinergic anti-inflammatory pathway (CAP), characterized by a significant decrease in tumor

28   necrosis factor α (TNF-α) upon LPS challenge. Using confocal microscopy we found that

29   induction of the CAP is associated with significant cytoplasmic retention of nuclear factor κB (NF-

30   κB). Co-cultures of human MDMs exposed to street RABV and autologous T cells further revealed

31   that the observed suppression of MDMs affects their function as T cell activators as well, as we

32   found a significant decrease in proliferation of CD8$^+$ T cells. Lastly, using flow cytometric analysis

33   we observed a significant increase in expression of CD163, hinting that street RABV is able to

34   polarize macrophages towards a M2-c anti-inflammatory phenotype. Taken together, these results

35   show that street RABV is capable of inducing an anti-inflammatory state in human macrophages,

36   which affects T cell proliferation.

Author summary

Rabies virus (RABV) is transmitted by a bite or a scratch from an infected animal. Infection leads to a lethal encephalitis and once clinical symptoms occur, there is no effective treatment available. The virus is able to travel from the initial site of infection to the central nervous system without triggering a strong immune response, using multiple mechanisms to evade and suppress the immune system. Up to present it is unclear when and where this immunosuppression is initiated, and if local immune cells are involved as well. Understanding the complete mechanisms of immunosuppression by RABV is essential for the development and improvement of effective post-exposure treatments. In this paper we studied if RABV is able to suppress human primary macrophages as these will be the first antigen-presenting cells that are recruited to the site of infection, and are known to be important in initiating an efficient immune response. We show that RABV is able to bind, but not infect, human macrophages. Binding induces an anti-inflammatory pathway, which leads to limited T cell proliferation and directs macrophages towards and anti-inflammatory state. These results show that RABV-macrophage interactions might indeed be one of the early steps in the onset of RABV-induced immunosuppression.

Introduction

Rabies is a zoonotic viral encephalitis responsible for 60 000 reported human deaths annually, although the true burden is suspected to be much higher (Hampson et al., 2015). The disease is caused by members of the genus *Lyssavirus*, -ssRNA viruses of the *Rhabdoviridae* family. While multiple lyssaviruses have been reported to cause rabies in humans, over 99 percent of all reported human cases are caused by dogs infected with rabies virus (RABV) (WHO, 2018). Nevertheless, in North and South America bats are the main source of human infections, mostly caused by silver-haired bat rabies virus (SHBRV) (Dietzschold et al., 2000).

While effective pre- and post-exposure prophylaxis is available, no treatment options are currently available once clinical symptoms occur. This makes rabies the deadliest zoonosis with a case-fatality rate approaching 100%. The virus is able to reach the CNS without triggering a strong local immune response (Schnell et al., 2010; Yamaoka et al., 2013); neither is a systemic immune response induced, as indicated by the low or absent neutralizing antibodies at the end-stage of disease of most patients (Kasempimolporn et al., 1991; Noah et al., 1998). This lack of immune activation is caused by limited viral replication at the inoculation site (Charlton et al., 1997; Murphy and Bauer, 1974), as well as by active immune evasion and suppression, as extensively reviewed (Katz et al., 2017; Scott and Nel, 2016). Previous research identified major immune evasive mechanisms, including the blocking of RIG-I activation by the nucleoprotein (N) (Masatani et al., 2013, 2011, 2010) and the IFN signal transduction pathway by the phosphoprotein (P) (Brzózka et al., 2006, 2005; Vidy et al., 2005).

To date, the majority of research on immunosuppressive mechanisms focused on the response in neurons and the CNS. While the absence of an effective local immune response after infection with RABV has been described (Yamaoka et al., 2013), it is not clear how exactly RABV affects local immune cells at the site of infection. Suppression of local immune cells may be responsible for the lack of immune response in later stages of diseases, hence increasing the knowledge on interactions between RABV and local immune cells is indispensable in the development of effective and targeted treatment strategies. Given this importance, we aimed to investigate the functional effects of street RABV on macrophages. Macrophages are versatile innate immune cells and play an essential role in the uptake and clearance of pathogens, and initiation of a strong local response by producing pro-inflammatory cytokines, chemokines and nitric oxide (NO) (Koh and

84   Dipietro, 2019; Mosser and Edwards, 2008). After being bitten or scratched by a rabid animal,

85   RABV first encounters resident macrophages in skin and muscle tissue, after which the inflicted

86   physical damage and the presence of bacteria and other microbes in the wound area induce a strong

87   influx of immune cells (Brancato and Albina, 2011; Daley et al., 2010). Large numbers of

88   infiltrated macrophages have been found in peripheral sites after inoculation with RABV as well

89   (Charlton and Casey, 1981); however, the interactions between RABV and macrophages have

90   been studied incompletely. The few studies focusing on the direct effects of RABV on

91   macrophages showed that various RABV strains were able to induce NO production and CXCL10

92   expression in RAW264 murine macrophages (Nakamichi et al., 2004), and induced macrophage

93   apoptosis through involvement of various caspases (Kip et al., 2017). In the aforementioned

94   papers, lab-adapted or attenuated RABV strains and murine macrophage-like cell lines were used,

95   therefore the effects of street RABV strains on primary macrophages remain unstudied.

96   Macrophages have a high functional plasticity. Upon encountering pathogens, and in combination

97   with cytokines produced by resident cells, macrophages polarize towards diverse and distinct

98   functional phenotypes, as are normally grouped into classically activated or inflammatory M1

99   phenotypes, and alternatively activated or anti-inflammatory M2 phenotypes (Stout et al., 2005).

100   A typical type 1/Th1 immune response, associated with M1 macrophages, aids the elimination of

101   intracellular pathogens while a typical type 2/Th2 response, associated with M2 macrophages, will

102   reduce viral clearance. Shifting macrophage polarization towards a phenotype beneficial for the

103   virus is a strategy known for many viruses, as extensively reviewed (Sang et al., 2015). Studies on

104   the effects of street RABV strains on macrophage polarization are lacking.

105   Nicotinic acetylcholine receptors (nAChr) are a family of ligand-gated pentameric ion channels

106   with a variety of pharmacological functions. The nAChr α7 is a homopentameric nAChr that

107   consists of five α7 subunits and is involved in the cholinergic anti-inflammatory pathway (CAP),

108   characterized by a decreased inflammatory response of macrophages upon binding of a typical

109   ligand (nicotine, acetylcholine) to nAChr α7 (Wang et al., 2003). RABV glycoprotein (RABV-G)

110   can bind to nAChr α7, but functional effects of this binding have not yet been studied (Kim et al.,

111   2010). We hypothesize that binding to the nAChr α7 leads to suppression of the inflammatory

112   response of macrophages.

113   In the present study we showed that a street RABV strain does not replicate in human monocyte-

114   derived macrophages (MDMs). We confirmed specific binding of RABV-G to nAChr α7 on

5

115   human MDMs and, for the first time, showed that a viral protein (RABV-G) was able to induce

116   the cholinergic anti-inflammatory pathway (CAP) in MDMs. We found that the induction of the

117   CAP was related to cytoplasmic retention of NF-κB in RABV-exposed MDMs, and that exposure

118   of MDMs with RABV decreased proliferation of autologous T cells *in vitro*. In parallel, exposure

119   of MDMs to RABV did not induce typical M1 phenotypic markers, but instead upregulated the

120   M2-c phenotypic marker CD163, hinting at the possibility that RABV is able to shift macrophage

121   polarization towards an anti-inflammatory M2-like phenotype.

122 **Methods**

123

124 **Virus**

125 A street rabies virus (RABV) strain known for its capability to cause human infections in North

126 America, the silver-haired bat rabies virus (SHBRV), was used. The virus was propagated in the

127 human neuroblastoma cell line SK-N-SH in Eagle's Minimum Essential Medium (EMEM) with

128 Earle's Balanced Salt Solution (EBSS) (Lonza), supplemented with 10% (v/v) Fetal Calf Serum

129 (FCS), 100 U penicillin (Gibco), 100 mg/mL streptomycin (Gibco), 2 mM L-glutamine (Gibco),

130 1% nonessential amino acids (Lonza), 1 mM sodium pyruvate (Gibco) and 1.5 mg/mL sodium

131 bicarbonate (Gibco). Virus titrations were performed by the median tissue culture infective dose

132 ($TCID_{50}$) endpoint dilution method of Reed and Muench (Reed and Muench, 1938) using the

133 mouse neuroblastoma cell line MNA. MNA cells were cultured in Dulbecco's Modified Eagle

134 Medium (DMEM, Gibco) supplemented with 10% FCS, 100U penicillin, 100 mg/mL

135 streptomycin, 2 mM L-glutamine and 1 mM sodium pyruvate (Gibco). SK-N-SH and MNA Cells

136 were maintained at 37 °C with 5% CO_2.

137

138 **Primary cell isolation and macrophage maturation**

139 Peripheral blood mononuclear cells (PBMCs) were isolated from buffy coats obtained from

140 healthy, non-smoking and non-rabies vaccinated individuals (Sanquin). PBMCs were obtained by

141 density centrifugation using Ficoll Paque PLUS (GE Healthcare). Monocytes and T cells were

142 obtained from PBMC fractions by magnetic associated cell sorting using $CD14^+$ and $CD3^+$ beads,

143 respectively, following manufacturers guidelines (Miltenyi Biotec). Purity of the sortings was

144 confirmed by flow cytometry using a BD Lyric flow cytometer (BD Biosciences).

145 Monocytes were seeded at a density of 100 000 cells per well in 96-well plates and were maturated

146 for six days in Roswel Park Memorial Institute-1640 (RPMI-1640) medium containing 10%

147 pooled human serum (Sanquin), 1% (v/v) GlutaMAX (Gibco) and 20 ng/mL monocyte colony-

148 stimulating factor (M-CSF, R&D Systems). Cells were maintained at 37 °C with 5% CO_2 and the

149 medium was replaced on day 2 and day 4.

150

151

152

Infection of human monocyte-derived macrophages

153

154 Mature human monocyte-derived macrophages, obtained on day six of culture, were exposed to

155 RABV for one hour in serum-free medium using a MOI of 0.1, 1, 10 or 50, after which the cells

156 were washed once and were incubated in complete medium. At 8, 24, 48, and 72 hours post-

157 infection, cell culture supernatants were harvested for virus titration and cells were fixed in 80 %

158 acetone for immunofluorescent detection of the nucleoprotein using a mouse FITC-labeled RABV-

159 N antibody (Fujirebio). Nuclear counterstaining with Hoechst 33342 (Sigma Aldrich) was

160 included before image acquisition using a Zeiss LSM700 confocal laser scanning microscope.

161 Virus titrations were performed by the $TCID_{50}$ endpoint dilutions method of Reed and Muench

162 using the mouse neuroblastoma cell line MNA, as described before. A total of six donors were

163 included for the MOIs 0.1 and 1, and two donors for the MOIs of 10 and 50. Two wells were

164 infected for every condition and all supernatants were titrated in triplicate. Infection of the highly

165 susceptible neuroblastoma cell lines SK-N-SH and MNA cells were included as positive controls

166 for virus infectiousness.

167

rRABV-tG binding assay

168

169 The ability of the RABV glycoprotein to bind to human monocyte-derived macrophages was

170 investigated using a recombinantly expressed trimeric form of RABV-G (rRABV-tG, described in

171 Koraka et al., 2014). rRABV-tG was labeled with a 0.1 mg/mL solution of FITC (Sigma Aldrich)

172 in 0.5M bicarbonate buffer (pH 9.5) for one hour under constant stirring, after which unbound

173 FITC was removed by overnight dialysis in PBS. Mature macrophages were incubated with 50

174 μg/mL FITC-labeled rRABV-tG for 30 minutes at 4 ºC. In parallel, macrophages were incubated

175 with ATTO-633 conjugated alpha-bungarotoxin (α-BTX; Alomone labs) or with an antibody

176 against the nicotinic acetylcholine receptor α7 (nAChr α7; Alomone Labs) followed by an

177 Alexa594 goat-anti-rabbit conjugate (Invitrogen). Nuclear counterstain with Hoechst 33342

178 (Sigma) was included before cells were imaged using a Zeiss LSM700 confocal laser scanning

179 microscope.

180 For quantification of rRABV-tG binding, mature macrophages (n=6 individual donors) were

181 detached using Accutase (Merck Millipore), blocked with 10% pooled human serum in PBS for

182 30 minutes and incubated with various concentrations of rRABV-tG (0-100 μg/mL) for 30 minutes

183 at 4 ºC. To verify the binding of rRABV-tG to the nAChr-α7, macrophages were incubated with

8

184 various concentrations of the nAChr α7 antagonist alpha-bungarotoxin (α-BTX, 0-50 ug/mL) for

185 15 minutes before addition of rRABV-tG. After two washes in FACS buffer, binding of rRABV-

186 tG, as well as the expression of nAChr α7 was quantified using a BD Lyric flow cytometer (BD

187 Biosciences). Data were analyzed using FlowJo V10.6.2.

188

Macrophage stimulation and TNF-α cytokine assay

190 The anti-inflammatory effect of RABV on macrophages was studied using a lipopolysaccharide

191 (LPS) stimulation. LPS is an outer membrane component of Gram-negative bacteria and is known

192 to induce a strong inflammatory response. Briefly, mature macrophages (n=6–9 donors) were

193 exposed to RABV (MOI of 10, 25 or 50) for one hour and subsequently with LPS (100 ng/mL) for

194 six hours. Treatment with acetylcholine (1 μg/mL) was used as a positive control for induction of

195 the cholinergic anti-inflammatory pathway. Wells without LPS challenge, or LPS challenge

196 without pre-exposure to infectious RABV or acetylcholine, were included as negative and positive

197 control, respectively. To confirm the binding of RABV to nAChr α7, the specific antagonist alpha-

198 bungarotoxin (α-BTX, 2 μg/mL) was used as a pre-treatment before cells were exposed to RABV

199 or acetylcholine, and subsequently to LPS (Fig 3A). All conditions were tested in triplicate wells.

200 Supernatants were collected after six hours of stimulation with LPS and TNF-α concentrations

201 were determined using the Legendplex TNF-α cytometric bead assay (BioLegend). Bead analysis

202 was performed by a BD FACS Lyric flow cytometer and the data was analyzed using FlowJo

203 V10.6.2. Relative TNF-α reduction per individual donor was obtained by normalizing MFI's

204 against the TNF-α production of the corresponding wells stimulated with LPS only.

205

Quantification of NF-κB nuclear translocation and retention

207 Macrophages (n=6 donors) were exposed to RABV (MOI of 50) or acetylcholine (1 μg/mL) and

208 afterwards challenged for six hours with LPS (100 ng/mL) as described above. Wells were washed

209 twice with PBS, fixed with 4% paraformaldehyde (PFA) in PBS for 15 minutes and permeabilized

210 using PBS 0.1% Triton X-100 for 15 minutes. After blocking for 30 minutes with 2% FCS in PBS,

211 wells were stained with a monoclonal antibody against the NF-κB the p65 subunit (Santa Cruz)

212 and goat-anti-mouse Alexa488 (Invitrogen). Nuclei were counterstained with Hoechst 33342

213 (Sigma Aldrich) and wells were imaged using a Zeiss LSM700 confocal laser scanning

214 microscope.

215   An ImageJ macro was designed to perform automatic and user-independent quantification of

216   nuclear and cytoplasmic NF-κB. Briefly, z-stacks were projected into single images by summing

217   the intensity of all slices. Nuclear regions were defined by the Hoechst 33342 staining and a binary

218   mask was created using an intensity threshold. Total NF-κB was detected by applying the Li

219   intensity threshold on the Alexa488 channel, after which the signal was converted into a binary

220   mask. In order to obtain the cytoplasmic NF-κB, the binary mask containing the nuclei was

221   subtracted from the total NF-κB channel. The area and mean NF-κB intensity were measured in

222   the original z-projection. Lastly, total NF-κB expression was determined by area * intensity of

223   both the nuclear and cytoplasmic region and the average nuclear/cytoplasmic ratios were

224   determined for each image. At least three high-magnification fields were imaged per well, and

225   nuclear/cytoplasmic ratios were determined for six donors in total.

226

227   **T cell co-culture**

228   Macrophages (n=6 donors) treated with RABV (MOI of 50) for one hour were washed twice with

229   medium (RPMI supplemented with10% FCS, 100U penicillin, 100 mg/mL streptomycin and 2

230   mM L-glutamine) before autologous T cells were added. $CD3^+$ T cells were stained with 2 μM

231   carboxyfluorescein succinimidyl ester (CFSE) as described before (Piazzon et al., 2015), were

232   activated with 2.5 μg/mL α-CD3 (Invitrogen) and α-CD28 (Invitrogen) and were co-cultured with

233   macrophages in a 1:1 ratio. Non-stimulated T cells, as well as stimulated T cells cultured without

234   macrophages, were taken along as controls for each donor. Cells were cultured in 3.5 days after

235   which proliferation was determined by flow cytometry. To this end, T cells were washed twice

236   with PBS, stained with the fixable viability dye ZombieViolet (Biolegend), fixed with 4% PFA for

237   15 minutes and subsequently stained for 30 minutes with anti-CD4-APC and anti-CD8-BV605

238   (Biolegend) in FACS buffer. Flow cytometry analysis was performed using a BD FACS Lyric

239   flow cytometer and the data were analyzed using FlowJo V10.6.2.

240

241   **Macrophage maturation and polarization**

242   Mature macrophages (n = 6 donors) were stimulated for 48 hours with complete medium

243   containing IFN-γ (20 ng/mL, R&D Systems) and LPS (100 ng/mL, Sigma Aldrich), with IL-4 (20

244   ng/mL, R&D Systems), or with IL-1 (20 ng/mL R&D Systems), to induce the M1, M2a or M2c

245   phenotype, respectively. To investigate the effect of rabies virus on macrophage polarization,

10

246   macrophages were stimulated with complete medium containing RABV (MOI of 10). Expression

247   of macrophage phenotypical markers was investigated by flow cytometry. Non-polarized

248   macrophages, cultured for 48 hours with complete medium without additional cytokines, were

249   taken along as controls for each donor.

250   Macrophages were dissociated from the wells using Accutase (Merck Millipore) and were washed

251   twice with PBS before staining for 30 minutes with the fixable viability dye ZombieViolet

252   (Biolegend). Cells were fixed with 4 % PFA for 15 minutes, and after Fc receptor blocking with

253   Human TruStain FcX (Biolegend), cells were stained with the following antibodies in FACS buffer

254   (PBS with 2 % fetal calf serum, 0.2 mM EDTA, 0.01% sodium azide): anti-CD80-FITC, anti-

255   HLA-DR-APC-Cy7, anti-PD-L1-APC, anti-CD163-PE, anti-CD200R-PE-Cy7 and anti-CD206

256   (BV786) (All Biolegend). Mean fluorescent intensities were quantified by flow cytometry using a

257   BD Lyric flow cytometer (BD Biosciences) and the data were analyzed using FlowJo V10.6.2.

258

259   **Statistical analysis**

260   All statistical analyses were performed using SPSS Statistics 25 (IBM).

261   For the rRABV-tG binding assay, the TNF-α cytokine assay and the polarization study, One-Way

262   ANOVAs were performed followed by Tukey's post-hoc tests to test significant differences

263   between treatments. For the NF-κB assay and the proliferation assay, paired sample T-tests were

264   performed to determine significant differences. P values < 0.05 were considered significant and

265   all results were expressed as mean ± SEM.

266   **Results**

267

268   **Street RABV does not replicate in human monocyte-derived macrophages**

269   To determine the immunomodulatory effects of RABV-macrophage interactions, we first

270   investigated if exposure to street RABV leads to a productive infection in human MDMs, measured

271   by an increase in virus over time. To this end, mature MDMs were exposed to street RABV in a

272   MOI of 0.1, 1, 10 or 50, and at 8, 24, 48, and 72 hours post-infection (hpi) the presence of virus

273   was examined by fluorescent microscopy and virus titration. The highly susceptible human

274   neuroblastoma cell lines MNA and SK-N-SH were taken along as positive controls. RABV-N

275   staining was detected from 24 hpi onwards in the MNA and SK-N-SH cells, but remained absent

276   throughout all time-points in the human MDMs (Fig 1A). MNA and SK-N-SH cells exposed to a

277   MOI of 1 reached a plateau phase around 48 hpi, with titers between $10^{6.17}$ and $10^{6.50}$ $TCID_{50}$/mL,

278   and cells inoculated with a MOI of 0.1 reached this phase around 72 hpi (Fig 1B). While a low

279   positive signal (10^1 $TCID_{50}$/mL) was detected at 24 hpi in human MDMs that were exposed to a

280   MOI of 1, no increase was observed at 48 and 72 hpi, or in MDMs infected with a higher MOI

281   This lack of increase of present virus, as well as the absence of RABV-N protein at all tested time

282   points, shows that inoculation with a street strain of RABV does not lead to a productive infection
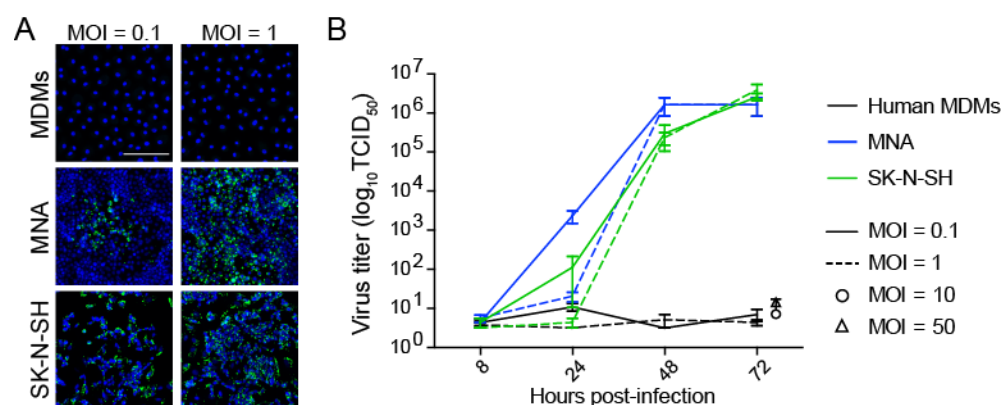
283   of mature human MDMs.

284

285

286

287   **Fig 1. Qualitative and quantitative assessment of the ability of RABV to infect mature human**

288   **monocyte-derived macrophages.** Human monocyte-derived macrophages (MDMs) were

289   exposed to street RABV at a MOI of 0.1, 1, 10 or 50, and at 72 hours post-infection (hpi) cells

290   were fixed and stained with an antibody against the RABV-N protein (A). The white scalebar

291   represents 500 μM and all images were acquired at the same magnification. In parallel,
292   supernatants of 8, 24, 48 and 72 hpi were titrated on MNA cells (B). Bars represent the mean ±
293   SEM of two-six donors; for each condition, two wells were infected per condition and all
294   supernatants were titrated in triplicate. Highly susceptible MNA and SK-N-SH cells were taken
295   along as positive controls.

296

297

298   **RABV glycoprotein binds to nAChr α7 on human monocyte-derived macrophages**

299   As a first step in testing if RABV is able to induce the cholinergic anti-inflammatory pathway

300   (CAP) in human macrophages, we investigated the ability of RABV-G to bind to nicotine

301   acetylcholine receptor alpha-7 subunit (nAChr α7) on human MDMs. Binding was examined by

302   both flow cytometry and confocal microscopy, using FITC-labelled recombinant trimeric RABV-

303   G (rRABV-G). First, expression of nAChr α7 was examined on mature MDMs by confocal

304   microscopy (Fig 2A) and flow cytometry (Fig 2B), confirming a strong expression of this receptor.

305   In parallel, investigation on the binding of nAChr α7 antagonist alpha-bungarotoxin (α-BTX) and

306   the FITC-labeled rRABV-tG by confocal microscopy, showed that both α-BTX and rRABV-tG

307   could efficiently bind to human MDMs (Fig 2A). Next, macrophages were incubated with various

308   concentrations of rRABV-tG, and flow cytometric analysis revealed a concentration-dependent

309   binding to the MDM surface (Fig 2C). In order to confirm that rRABV-tG binds to nAChr α7, a

310   pre-treatment with α-BTX was used. Although no significant inhibition of rRABV-tG binding was

311   observed at any of the tested α-BTX concentrations (0-50 μg/mL), binding showed a decreasing

312   trend with increasing concentrations of α-BTX (Fig 2C). This confirms that α-BTX and rRABV-

313   tG compete for the same receptor and that indeed rRABV-tG binds to nAChr α7 on human MDMs.
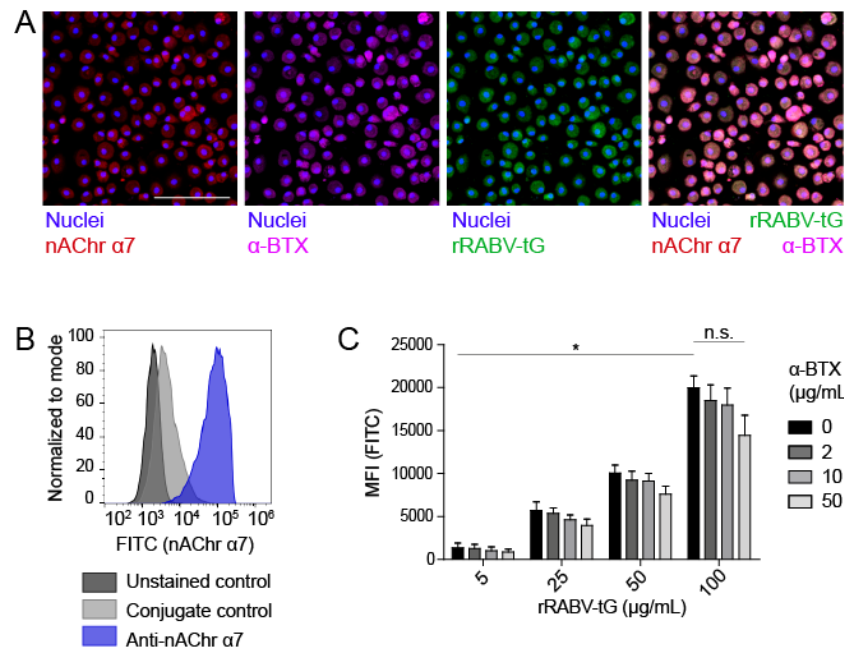
Fig 2. Presence of nAChr α7 on mature human monocyte-derived macrophages and binding of recombinant trimeric RABV glycoprotein to this receptor. (A) The presence of nAChr α7 on mature human MDMs, as well as the binding of α-BTX and FITC-labeled rRABV-tG was visualized by confocal laser scanning microscopy. Nuclei were stained with Hoechst 33342. The white scalebar represents 500 μM. The rightmost plot shows an overlaid image of the nAChr α7 staining and α-BTX and rRABV-tG binding. Presence of nAChr α7 was confirmed by flow cytometry (B) and this technique was also used to quantify binding of FITC-labeled rRABV-tG, shown by the mean-fluorescent intensity (MFI) of the FITC channel representing rRABV-tG binding, as well as the blocking of binding by pre-incubation with the nAChr α7 specific antagonist α-BTX (C). Bars represent the mean ± SEM for a total of six donors. *P* values < 0.05 were considered significant and are indicated with an asterisk (*). Non-significant comparisons were indicated with n.s.

Binding of RABV to nAChr α7 induces the cholinergic anti-inflammatory pathway in human macrophages through cytoplasmic retention of NF-κB

After confirming that rRABV-tG binds to nAChr α7 on human macrophages we set out to investigate whether this binding could result in induction of the cholinergic anti-inflammatory pathway (CAP). Mature MDMs were exposed to various doses of RABV (MOI = 10, 25, 50), after which they were stimulated with LPS for six hours. Quantification of TNF-α by cytometric bead assays showed that exposure to high concentrations of RABV (MOI of 50) resulted in a significant decrease in TNF-α upon stimulation with LPS (Fig 3A). The decrease in TNF-α production (30.1

14

337   % on average) was similar to the decrease observed with wells pre-treated with acetylcholine, a

338   prototypical ligand of nAChr α7. The lower concentrations of RABV (MOI of 10 and 25) did not

339   induce this decrease, indicating that higher viral concentrations were required to induce the CAP.

340   Importantly, by pre-treating macrophages with α-BTX we were able to inhibit the induction of the

341   CAP, as TNF-α production was similar to the controls treated with LPS only. This confirms that

342   observed induction of the CAP is caused by specific binding of RABV-G to nAChr α7.

343   Next, we aimed at investigating whether induction of the CAP by RABV also involves cytoplasmic

344   retention of NF-κB, as is described for the prototypical ligands nicotine and acetylcholine.

345   Macrophages were either treated with RABV (MOI of 50) or acetylcholine before challenge with

346   LPS, after which the cells were fixed and stained with an antibody against the NF-κB p65 subunit.

347   Nuclear and cytoplasmic NF-κB were quantified in confocal microscopy images using ImageJ

348   batch image processing. Exposure of human MDMs to LPS led to nuclear translocation of NF-κB,

349   hereby significantly increasing the nuclear/cytoplasmic ratio (Fig 3B and 3C). This translocation

350   could be blocked almost completely by pre-treating macrophages with RABV or acetylcholine,

351   causing cytoplasmic retention of NF-κB. Notably, the cytoplasmic retention caused by both RABV

352   and acetylcholine could be blocked by pre-treating the cells with the nAChr α7 specific antagonist

353   α-BTX, confirming that binding of RABV to the nAChr α7 is essential for the observed NF-κB
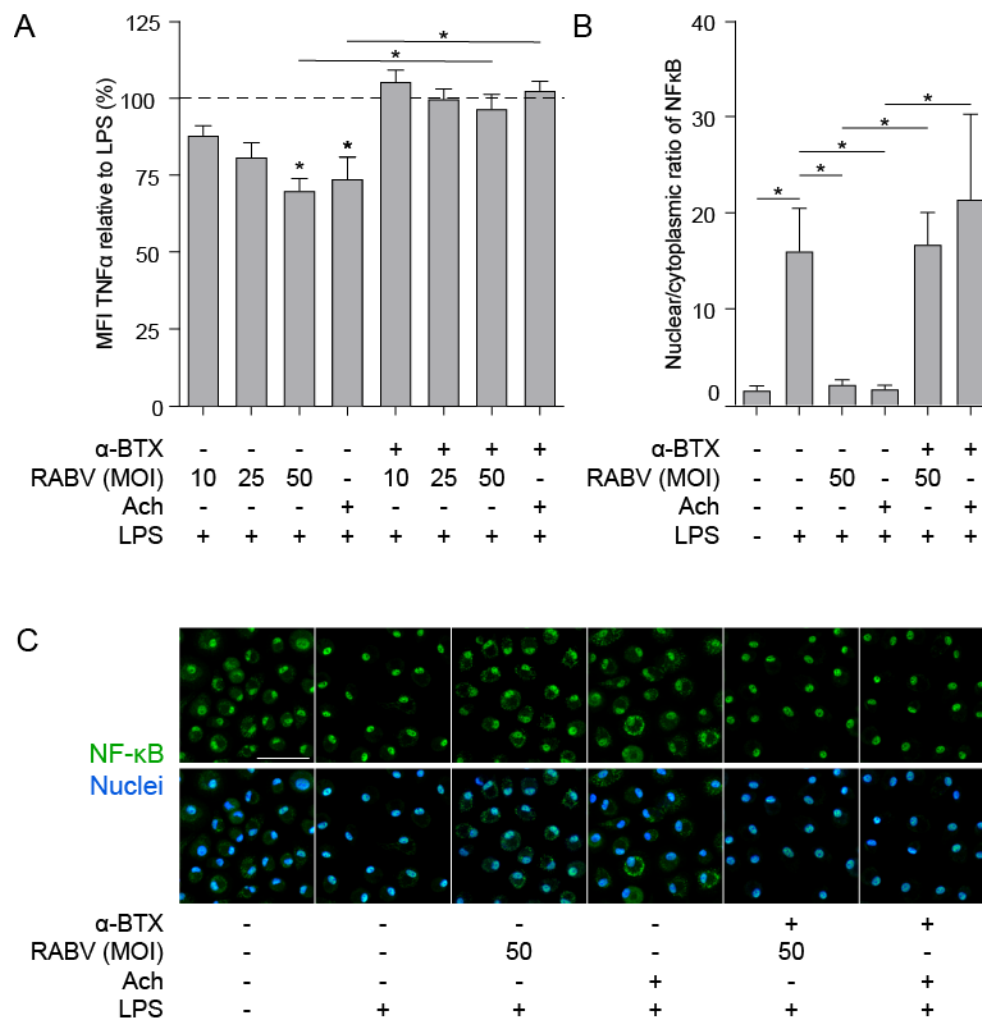
354   cytoplasmic retention.

Fig 3. Quantification of the anti-inflammatory effect induced of RABV on human macrophages and the role of cytoplasmic retention of NF-κB. (A) TNF-α production in human macrophages after six hours stimulation with LPS (100 ng/mL), with ('+') or without ('-') pre-treatment of α-BTX (2 μg/mL), RABV or acetylcholine (Ach; 1 μM), or a combination. Bars represent the mean ± SEM of TNF-α normalized to cells stimulated with LPS only (positive control, dotted horizontal line) for each individual donor (n = 6–9). Horizontal lines represent paired comparisons, whereas asterisks without horizontal lines indicate comparisons with the positive control (LPS only). (B) Nuclear and cytoplasmic NF-κB was quantified by image analysis in ImageJ using a batch image analysis. Bars represent the mean ± SEM of six donors, for which three high-magnification fields were analyzed per treatment. *P* values < 0.05 were considered significant and are indicated with an asterisk (*). Representative pictures of NF-κB staining are depicted in panel (C). Pictures where the NF-κB staining (green) completely overlaps with the nuclei (blue) show full nuclear translocation, whereas pictures with non-complete overlap of NF-κB and nuclei indicate cytoplasmic retention of NF-κB. The white scalebar represents 500 μM and all images were acquired at the same magnification.

16

RABV-exposed macrophages suppress T cell proliferation

Macrophages play an important role in initiating adaptive immune responses by presenting antigens and producing various cytokines that either inhibit or activate T proliferation upon interaction with these cells. We investigated if the observed anti-inflammatory response of RABV on human MDMs could also affect T cell proliferation *in vitro*. To study this, we performed co-cultures of macrophages exposed to RABV (MOI of 50), and autologous T cells that had been activated with soluble α-CD3 and α-CD28. T cells were stained with CFSE, and after 3.5 days T cell proliferation was analyzed by flow cytometry. Proliferation of CD8$^+$ T cells was significantly decreased upon co-culture with RABV-exposed macrophages (average decrease of 8.6 %) when compared to T cells cultured with control macrophages not exposed to RABV (Fig 4). Although not significant, CD4$^+$ T cells showed a similar trend (average decrease of 7.8 %). This shows that exposure of human MDMs to RABV is able to suppress T cell proliferation *in vitro*.
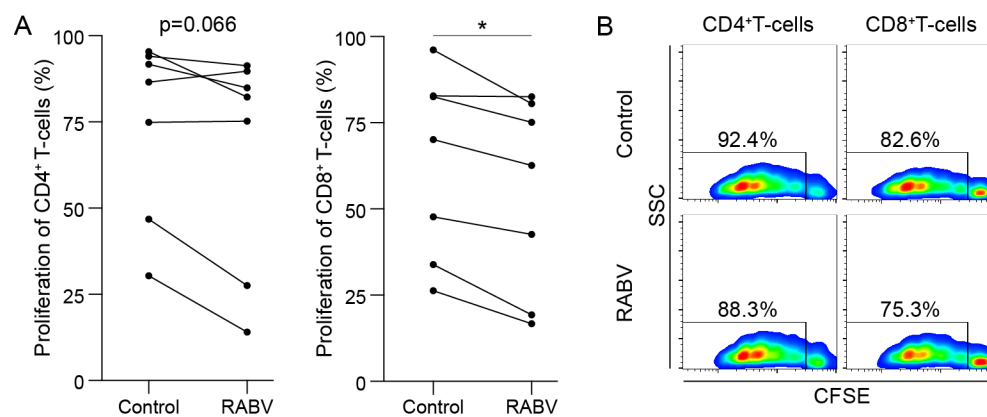

Fig 4. Proliferation of autologous T cells during *in vitro* co-culture with human monocyte-derived macrophages exposed to RABV. Proliferation of CFSE-stained T cells was quantified by flow cytometry after 3.5 days of co-culture with autologous MDMs previously exposed to RABV (MOI = 50). T cells cultured in the presence of macrophages that were not exposed to RABV were taken along as controls. Individual donors (n = 6) are shown in (A) and representative CFSE plots showing the fluorescent intensity and percentages of proliferation are shown in (B). *P* values < 0.05 were considered significant and are indicated with an asterisk (*).

397   **RABV does not polarize human macrophages towards a M1 phenotype but induces**

398   **upregulation of the M2-c marker CD163**

399   After showing that exposure to RABV induces an anti-inflammatory pathway in human MDMs,

400   we investigated whether longer exposure (48 hours) to RABV (MOI of 10) was able to induce

401   polarization of human MDMs. A panel of M1, M2-a and M2-c phenotypical markers was used to

402   investigate the macrophages' phenotype by flow cytometry; polarizing cytokine cocktails known

403   to induce M1, M2-a and M2-c phenotypes were taken along as controls. Polarization with IFN-γ

404   and LPS induced a typical M1 phenotype, characterized by significant upregulation of CD80,

405   HLA-DR and PD-L1 (Fig 5). Contrary to this, the typical M2-a markers CD200R and CD206 were

406   upregulated after polarization with IL1-4. CD163, a typical M2-c marker, was not only upregulated

407   after polarization with IL-10, but also after exposure to RABV. Although PD-L1 was also

408   upregulated in macrophages polarized in the presence of RABV, the upregulation was lower than

409   observed in macrophages polarized with IL-4. All together these findings demonstrate that while

410   RABV does not induce a typical M1 phenotype, it might steer macrophage polarization towards

411   an M2-c phenotype, as characterized by the upregulation of CD163.
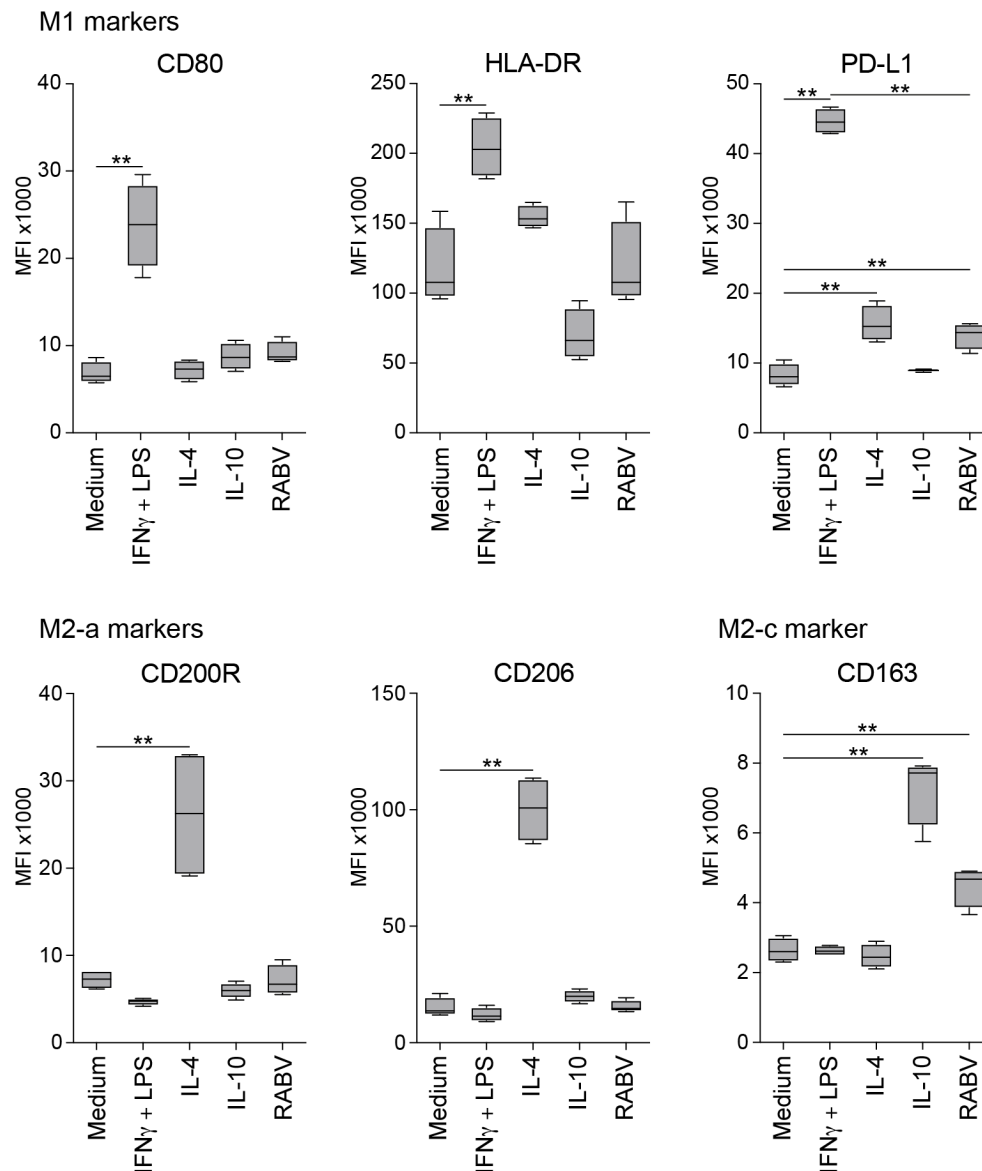
412

413

414

Fig 5. Expression levels of macrophage phenotypical markers after 48 hours of polarization with various cytokines or RABV. Panels represent typical M1 markers (CD80, HLA-DR and PD-L1), M2-a markers (CD200R and CD206) and the M2-c marker CD163. Mean fluorescent intensities (MFI) were measured by flow cytometry after 48 hours of polarization. Bars represent the mean ± SEM of six donors. Values were considered significant when $P < 0.05$ and are indicated with an asterisk (*). $P < 0.005$ are indicated with (**).

Discussion

421

422

423 In this study we investigated if street RABV can induce anti-inflammatory pathways in human

424 MDMs and if interaction between RABV and macrophages can affect T cell proliferation.

425 Knowledge on the early interactions between RABV and local immune cells are of utmost

426 importance in order to develop and improve efficient post-exposure treatments. We demonstrate

427 that a street RABV strain (SHBRV) has an anti-inflammatory effect on human MDMs by inducing

428 the CAP through binding of RABV-G to nAChr α7, characterized by cytoplasmic retention of NF-

429 κB and a decreased TNF-α response upon LPS stimulation. We further show that exposure of

430 macrophages to RABV decreases T cell proliferation *in vitro* and upregulates surface expression

431 of CD163, a marker of the anti-inflammatory M2-c phenotype.

432 Before studying the immunomodulatory effects of street RABV on human MDMs, we investigated

433 if street RABV is able to replicate in human MDMs and concluded that this is not the case (Fig 1).

434 This lack of replication was also reported in murine bone marrow- or peritoneal-derived

435 macrophages infected with various street RABV strains (Ray et al., 1995), indicating that primary

436 macrophages are non-permissive to infection with street RABV strains. In contrast, primary

437 murine macrophages did show replication of the lab-adapted CVS-11 and attenuated HEP Flury

438 strains (Kip et al., 2017) and the recombinant matrix gene-deleted vaccine strain rRABV-ΔM

439 (Lytle et al., 2015). This indicates that in contrast to street RABV strains, some attenuated strains

440 are able to productively infect primary macrophages.

441 We next confirmed that RABV-G specifically binds to the nAChr α7 on human MDMs, as binding

442 of the recombinant trimeric rRABV-tG was decreased when cells were pre-treated with the

443 receptor-specific antagonist α-BTX. However, pre-treatment did not block binding of rRABV-tG

444 completely, indicating that RABV-G binds to other receptors on human MDMs as well.

445 Alternative receptors may include additional nAChr, given that the expression of a wide array of

446 nAChr (including α1, α-3-6, α9-10, β1-β4) have been described for human macrophages and

447 macrophage-like cell lines (Chernyavsky et al., 2010; Galvis et al., 2006).

448 While major immune evasive mechanisms have been identified for the RABV nucleoprotein (N)

449 and phosphoprotein (P), affecting RIG-I activation (Masatani et al., 2013, 2011, 2010) and the IFN

450 signal transduction pathway (Brzózka et al., 2006, 2005; Vidy et al., 2005) or cytokine signaling

451 (Harrison et al., 2020) respectively, related mechanisms for the surface protein RABV-G have not

20

452   yet been identified. Our results show that exposure of human MDMs to RABV leads to a decreased

453   TNF-α response upon LPS challenge, caused by cytoplasmic retention of NF-κB. TNF-α levels

454   and NF-κB nuclear translocation was completely restored when MDMs were pre-treated with the

455   nAChr α7-specific antagonist α-BTX, showing that the observed anti-inflammatory effects of

456   RABV were caused by binding of the RABV-G to nAChr α7. While multiple molecules have been

457   found to induce the CAP in macrophages, including GTS-21 (van Westerloo et al., 2006), CAP55

458   (Saeed et al., 2005) and PNU-282987 (Dash et al., 2016), to our knowledge this is the first study

459   showing that a viral protein is able to induce this pathway. The CAP might have additional effects

460   on RABV pathogenesis and disease development, as was shown that the nAChr α7 antagonist

461   GTS-21 attenuates the cytokine response in monocytes after stimulation with ligands for Toll-Like

462   Receptor 2 (TLR2), TLR3, TLR4, TLR9 and RAGE. Furthermore, downregulating the

463   inflammatory response was also observed in microglia (Egea et al., 2015), which are resident CNS

464   macrophages that also express nAChr-α7 (Shytle et al., 2004).

465   Given the importance of the NF-κB signaling pathway in the initiation of an immune response,

466   multiple viruses (including Borna disease virus, Epstein-Barr virus, Hantaan virus, Hepatitis C

467   virus, Poliovirus, Varicella-zoster virus and West Nile virus, as extensively reviewed (Rahman

468   and McFadden, 2011)) have acquired mechanisms to inhibit NF-κB activation. We showed that

469   RABV induced cytoplasmic retention of NF-κB *in vitro*, which is described as an essential step in

470   activation of the CAP (Wang et al., 2004). For RABV it is known that the matrix (M) protein is

471   able to inhibit RelAP43 activation, a splice variant of the NF-κB subunit RelA, leading to

472   decreased expression of various innate immune genes (Benoit et al., 2017; Khalifa et al., 2016;

473   Luco et al., 2012). Similar effects have not yet been described for the other RABV proteins and

474   our study is the first to show that RABV-G is able to specifically inhibit activation of the NF-κB

475   signaling pathway. Contrary to our findings, microglia-like cell lines infected with the attenuated

476   strain CVS-11 showed a strong activation of NF-κB (Nakamichi et al., 2005). However, productive

477   infection was observed in the cell lines used in that study.

478   Macrophages are APCs and potent cytokine producing cells, and therefore suppressed macrophage

479   functioning can lead to decreased T cell activation. T cell activation requires three signals: T cell

480   receptor (TCR) binding to antigens presented on major histocompatibility complexes (MHC) of

481   APCs (signal 1), binding of costimulatory molecules (signal 2), and activation by cytokines. It has

482   been proposed that IL-1 can provide the third signal for CD4^{+} cells (Curtsinger and Mescher, 2010;

21

483   Huber et al., 1998), resulting in T cell activation. Given that the inhibition of IL-1 had been

484   described after induction of the CAP in macrophages (Sugano et al., 1998; Takahashi et al., 2006)

485   the observed decrease in T cell proliferation might be caused by a decreased activation of $CD4^+$ T

486   cells. As a consequence, decreased cytokine production by $CD4^+$ cells, and especially IL-2, can be

487   a probable explanation for the significant decrease in $CD8^+$ T cell proliferation.

488   Viral antigens can be sensed by macrophages and are capable of steering macrophage polarization

489   in a certain direction (Brancato and Albina, 2011; Daley et al., 2010); the classically activated M1,

490   or pro-inflammatory macrophage, and the M2 macrophage, also known as alternatively activated

491   or anti-inflammatory macrophages (Koh and Dipietro, 2019; Mosser and Edwards, 2008).

492   Generally, macrophages polarize towards an M1 phenotype after recognition of intracellular

493   pathogens, including viruses. We showed that exposure of human MDMs to a street RABV strain

494   for 2 days significantly upregulated the M2-c marker CD163, while the typical M1-markers CD80

495   and HLA-DR remained unchanged. While more in-depth investigation on surface marker

496   expression and macrophage functioning is necessary, the results hint at the ability of street RABV

497   to shift macrophage polarization towards an M2-c phenotype. Studies on the effects of street

498   RABV strains on polarization of primary macrophages are lacking, but studies using attenuated

499   viruses CVS-11 and HEP show an opposite effect. Upregulated gene expression of iNOS and nitric

500   oxide (NO) expression, a key characteristic of M1 macrophages, in the murine macrophage-like

501   cell like RAW264 (Nakamichi et al., 2004), and the attenuated SPBN-GAS was able to shift the

502   polarization pattern of tumor-associated macrophages (TAMs), that normally resemble a M2-

503   phenotype, towards an M1-phenotype in glioma-bearing mice (Bongiorno et al., 2017).

504   CD163 is a scavenger receptor within the cysteine-rich family and is a marker of M2-c anti-

505   inflammatory macrophages. Increased CD163 expression on macrophages has been reported

506   during viral hepatitis (Hiraoka et al., 2005), and infection of pigs with porcine reproductive and

507   respiratory syndrome virus (Patton et al., 2009) and African swine fever virus (Sánchez-Torres et

508   al., 2003). Furthermore, an increase in $CD163^+$ macrophages was found in individuals infected

509   with human immunodeficiency virus type 1 (Fischer-Smith et al., 2008), as well as in rhesus

510   macaques infected with simian immunodeficiency virus (Yearley et al., 2007). Interestingly, the

511   latter study showed a negative correlation between $CD163^+$ macrophages and inflammatory

512   infiltration in areas infected, indicating that $CD163^+$ macrophages serve an anti-inflammatory or

513   immunosuppressive role. In addition, $CD163^+$ TAMs were found to suppress T cell proliferation

514   in several disease models (Han et al., 2016; Lepique et al., 2009; Lievense et al., 2016; Oishi et

515   al., 2016).

516   In summary, our results show for the first time that a viral protein, the RABV-G of a street RABV

517   strain, is able to induce the CAP in human MDMs. We show that this anti-inflammatory pathway

518   is induced by binding of RABV-G to nAChr α7, using the specific antagonist α-BTX, leading to

519   cytoplasmic retention of NF-κB. Besides the decreased inflammatory response upon challenge

520   with LPS we found that exposing human MDMs to RABV leads to suppression of T cell

521   proliferation *in vitro*. We also show that exposure of human MDMs to RABV does not induce a

522   typical, inflammatory M1 phenotype, but instead a significant upregulation of CD163, marker of

523   a M2-c anti-inflammatory phenotype. Given that the absence of a strong local innate immune

524   response is beneficial for the virus, polarizing resident and infiltrating macrophages towards an

525   anti-inflammatory M2-c phenotype might be another mechanism of RABV to evade the immune

526   system.

527   Future studies should focus on further understanding of the observed lack of adaptive immune

528   response. Additional *in vitro* experiments in which the effects of "RABV-polarized" macrophages

529   on T and B cells are investigated will allow evaluation of the role of macrophage suppression on

530   the lack of neutralizing antibodies in RABV patients. *In vivo* experiments using targeted transgenic

531   mice will allow reveal the role of macrophage suppression on the complete course of disease.

532   Altogether, thorough insights into the different mechanisms that RABV uses to suppress the

533   immune system are essential for the development of new and improved PEP and treatment options

534   in RABV infection.

535 **Acknowledgements**

536

540 **References**

541

542 Benoit, B., Sonthonnax, F., Duchatea, M., Khalifa, Y. Ben, Larrous, F., Eun, H., Hourdel, V.,
543   Matondo, M., Chamot-Rooke, J., Grailhe, R., Bourhy, H., 2017. Regulation of NF-kB by
544   the p105-ABIN2-TPL2 complex and RelAp43 during rabies virus infection. PLoS Pathog.
545   1–24.

546 Bongiorno, E.K., Garcia, S.A., Sauma, S., Hooper, D.C., 2017. Type 1 Immune Mechanisms
547   Driven by the Response to Infection with Attenuated Rabies Virus Result in Changes in the
548   Immune Bias of the Tumor Microenvironment and Necrosis of Mouse GL261 Brain
549   Tumors. J. Immunol. 198, 4513–4523. doi:10.4049/jimmunol.1601444

550 Brancato, S.K., Albina, J.E., 2011. Wound Macrophages as Key Regulators of Repair. Am. J.
551   Pathol. 178, 19–25. doi:10.1016/j.ajpath.2010.08.003

552 Brzózka, K., Finke, S., Conzelmann, K.-K., 2006. Inhibition of Interferon Signaling by Rabies
553   Virus Phosphoprotein P: Activation-Dependent Binding of STAT1 and STAT2. J. Virol. 80,
554   2675–2683. doi:10.1128/jvi.80.6.2675-2683.2006

555 Brzózka, K., Finke, S., Conzelmann, K.-K., 2005. Identification of the rabies virus alpha/beta
556   interferon antagonist: phosphoprotein P interferes with phosphorylation of Interferon
557   Regulatory factor 3. J. Virol. 79, 7673–7681. doi:10.1128/JVI.79.12.7673

558 Charlton, K.M., Casey, G.A., 1981. Experimental rabies in skunks: persistence of virus in
559   denervated muscle at the inoculation site. Can. J. Comp. Med. 45, 357–362.

560 Charlton, K.M., Nadin-Davis, S., Casey, G.A., Wandeler, A.I., 1997. The long incubation period
561   in rabies: Delayed progression of infection in muscle at the site of exposure. Acta
562   Neuropathol. 94, 73–77. doi:10.1007/s004010050674

563 Chernyavsky, A.I., Arredondo, J., Skok, M., Grando, S.A., 2010. Auto/paracrine control of
564   inflammatory cytokines by acetylcholine in macrophage-like U937 cells through nicotinic
565   receptors. Int. Immunopharmacol. 10, 308–315. doi:10.1016/j.intimp.2009.12.001

566 Curtsinger, J.M., Mescher, M.F., 2010. Inflammatory cytokines as a third signal for T cell
567   activation. Curr. Opin. Immunol. 22, 333–340. doi:10.1038/jid.2014.371

568 Daley, J.M., Brancato, S.K., Thomay, A.A., Reichner, J.S., Albina, J.E., 2010. The phenotype of
569   murine wound macrophages. J. Leukoc. Biol. 87, 59–67. doi:10.1189/jlb.0409236

570 Dash, P.K., Zhao, J., Kobori, N., Redell, J.B., Hylin, M.J., Hood, K.N., Moore, A.N., 2016.

571   Activation of alpha 7 cholinergic nicotinic receptors reduce blood–brain barrier

572   permeability following experimental traumatic brain injury. J. Neurosci. 36, 2809–2818.

573   doi:10.1523/JNEUROSCI.3197-15.2016

574 Dietzschold, B., Morimoto, K., Hooper, D.C., Smith, J.S., Rupprecht, C.E., Koprowski, H.,

575   2000. Genotypic and phenotypic diversity of rabies virus variants involved in human rabies:

576   implications for postexposure prophylaxis. J. Hum. Virol. 3, 50–57.

577 Egea, J., Buendia, I., Parada, E., Navarro, E., León, R., Lopez, M.G., 2015. Anti-inflammatory

578   role of microglial alpha7 nAChRs and its role in neuroprotection. Biochem. Pharmacol. 97,

579   463–472. doi:10.1016/j.bcp.2015.07.032

580 Fischer-Smith, T., Tedaldi, E.M., Rappaport, J., 2008. CD163/CD16 coexpression by circulating

581   monocytes/macrophages in HIV: Potential biomarkers for HIV infection and AIDS

582   progression. AIDS Res. Hum. Retroviruses 24, 417–421. doi:10.1089/aid.2007.0193

583 Galvis, G., Lips, K.S., Kummer, W., 2006. Expression of nicotinic acetylcholine receptors on

584   murine alveolar macrophages. J. Mol. Neurosci. 30, 107. doi:10.1385/JMN/30:1-2:107

585 Hampson, K., Coudeville, L., Lembo, T., Sambo, M., Kieffer, A., Attlan, M., Barrat, J., Blanton,

586   J.D., Briggs, D.J., Cleaveland, S., Costa, P., Freuling, C.M., Hiby, E., Knopf, L., Leanes, F.,

587   Meslin, F.X., Metlin, A., Miranda, M.E., Müller, T., Nel, L.H., Recuenco, S., Rupprecht,

588   C.E., Schumacher, C., Taylor, L., Vigilato, M.A.N., Zinsstag, J., Dushoff, J., 2015.

589   Estimating the Global Burden of Endemic Canine Rabies. PLoS Negl. Trop. Dis. 9, 1–20.

590   doi:10.1371/journal.pntd.0003709

591 Han, Q., Shi, H., Liu, F., 2016. CD163 + M2-type tumor-associated macrophage support the

592   suppression of tumor-infiltrating T cells in osteosarcoma. Int. Immunopharmacol. 34, 101–

593   106. doi:10.1016/j.intimp.2016.01.023

594 Harrison, A.R., Lieu, K.G., Larrous, F., Ito, N., Bourhy, H., Moseley, G.W., 2020. Lyssavirus P-

595   protein selectively targets STAT3- STAT1 heterodimers to modulate cytokine signalling.

596   PLoS Pathog. 1–23. doi:10.1371/journal.ppat.1008767

597 Hiraoka, A., Horiike, N., Fazle Akbar, S.M., Michitaka, K., Matsuyama, T., Onji, M., 2005.

598   Expression of CD163 in the liver of patients with viral hepatitis. Pathol. Res. Pract. 201,

599   379–384. doi:10.1016/j.prp.2004.10.006

600 Huber, M., Beuscher, H.U., Rohwer, P., Kurrle, R., Röllinghoff, M., Lohoff, M., 1998.

601   Costimulation via TCR and IL-1 receptor reveals a novel IL-1α-mediated autocrine pathway

602   of TH2 cell proliferation. J. Immunol. 160, 4242–4247.

603 Kasempimolporn, S., Hemachudha, T., Khawplod, P., Manatsathit, S., 1991. Human immune

604   response to rabies nucleocapsid and glycoprotein antigens. Clin. Exp. Immunol. 84, 195–

605   199. doi:10.1111/j.1365-2249.1991.tb08148.x

606 Katz, I.S.S., Guedes, F., Fernandes, E.R., Dos Ramos Silva, S., 2017. Immunological aspects of

607   rabies: a literature review. Arch. Virol. 162, 1–18. doi:10.1007/s00705-017-3484-0

608 Khalifa, Y. Ben, Luco, S., Besson, B., Sonthonnax, F., Archambaud, M., Grimes, J.M., Larrous,

609   F., Bourhy, H., 2016. The matrix protein of rabies virus binds to RelAp43 to modulate NF-

610   κB-dependent gene expression related to innate immunity. Sci. Rep. 6, 1–13.

611   doi:10.1038/srep39420

612 Kim, S.-S., Ye, C., Kumar, P., Chiu, I., Subramanya, S., Wu, H., Shankar, P., Manjunath, N.,

613   2010. Targeted Delivery of siRNA to Macrophages for Anti-inflammatory Treatment. Mol.

614   Ther. 18, 993–1001. doi:10.1038/mt.2010.27

615 Kip, E., Nazé, F., Suin, V., Vanden Berghe, T., Francart, A., Lamoral, S., Vandenabeele, P.,

616   Beyaert, R., Van Gucht, S., Kalai, M., 2017. Impact of caspase-1/11, -3, -7, or IL-1β/IL-18

617   deficiency on rabies virus-induced macrophage cell death and onset of disease. Cell Death

618   Discov. 3, 17012. doi:10.1038/cddiscovery.2017.12

619 Koh, T.J., Dipietro, L.A., 2019. Inflammation and wound healing : the role of the macrophage.

620   Expert Rev. Mol. Med. 13, 1–12. doi:10.1017/S1462399411001943

621 Koraka, P., Bosch, B.J., Cox, M., Chubet, R., Amerongen, G. van, Lövgren-Bengtsson, K.,

622   Martina, B.E.E., Roose, J., Rottier, P.J.M., Osterhaus, A.D.M.E., 2014. A recombinant

623   rabies vaccine expressing the trimeric form of the glycoprotein confers enhanced

624   immunogenicity and protection in outbred mice. Vaccine 32, 4644–4650.

625   doi:10.1016/j.vaccine.2014.06.058

626 Lepique, A.P., Daghastanli, K.R.P., Cuccovia, I., Villa, L.L., 2009. HPV16 tumor associated

627   macrophages suppress antitumor T cell responses. Clin. Cancer Res. 15, 4391–4400.

628   doi:10.1158/1078-0432.CCR-09-0489

629 Lievense, L.A., Cornelissen, R., Bezemer, K., Kaijen-Lambers, M.E.H., Hegmans, J.P.J.J., Aerts,

630   J.G.J.V., 2016. Pleural effusion of patients with malignant mesothelioma induces

631   macrophage-mediated T Cell suppression. J. Thorac. Oncol. 11, 1755–1764.

632   doi:10.1016/j.jtho.2016.06.021

633   Luco, S., Delmas, O., Vidalain, P.O., Tangy, F., Weil, R., Bourhy, H., 2012. RelAp43, a Member

634   of the NF-κB Family Involved in Innate Immune Response against Lyssavirus Infection.

635   PLoS Pathog. 8. doi:10.1371/journal.ppat.1003060

636   Lytle, A.G., Shen, S., McGettigan, J.P., 2015. Lymph node but not intradermal injection site

637   macrophages are critical for germinal center formation and antibody responses to rabies

638   vaccination. J. Virol. 89, 2842–8. doi:10.1128/JVI.03409-14

639   Masatani, T., Ito, N., Ito, Y., Nakagawa, K., Abe, M., Yamaoka, S., Okadera, K., Sugiyama, M.,

640   2013. Importance of rabies virus nucleoprotein in viral evasion of interferon response in the

641   brain. Microbiol. Immunol. 57, 511–517. doi:10.1111/1348-0421.12058

642   Masatani, T., Ito, N., Shimizu, K., Ito, Y., Nakagawa, K., Abe, M., Yamaoka, S., Sugiyama, M.,

643   2011. Amino acids at positions 273 and 394 in rabies virus nucleoprotein are important for

644   both evasion of host RIG-I-mediated antiviral response and pathogenicity. Virus Res. 155,

645   168–174. doi:10.1016/j.virusres.2010.09.016

646   Masatani, T., Ito, N., Shimizu, K., Ito, Y., Nakagawa, K., Sawaki, Y., Koyama, H., Sugiyama,

647   M., 2010. Rabies Virus Nucleoprotein Functions To Evade Activation of the RIG-I-

648   Mediated Antiviral Response. J. Virol. 84, 4002–4012. doi:10.1128/jvi.02220-09

649   Mosser, D.M., Edwards, J.P., 2008. Exploring the full spectrum of macrophage activation. Nat.

650   Rev. Immunol. 8, 958–969. doi:10.1038/nri2448

651   Murphy, A.M., Bauer, S.P., 1974. Early street rabies virus infection in striated muscle and later

652   progression to the central nervous system. Intervirology 3, 256–268.

653   Nakamichi, K., Inoue, S., Takasaki, T., Morimoto, K., Kurane, I., 2004. Rabies Virus Stimulates

654   Nitric Oxide Production and CXC Chemokine Ligand 10 Expression in Macrophages

655   through Activation of Extracellular Signal-Regulated Kinases 1 and 2. J. Virol. 78, 9376–

656   9388. doi:10.1128/JVI.78.17.9376

657   Nakamichi, K., Saiki, M., Sawada, M., Yamamuro, Y., Morimoto, K., Kurane, I., Takayama-ito,

658   M., 2005. Rabies Virus-Induced Activation of Mitogen-Activated Protein Kinase and NF- κ

659   B Signaling Pathways Regulates Expression of CXC and CC Chemokine Ligands in

660   Microglia. J. Virol. 79, 11801–11812. doi:10.1128/JVI.79.18.11801

661   Noah, D.L., Drenzek, C.L., Smith, J.S., Krebs, J.W., Orciari, L., Shaddock, J., Sanderlin, D.,

662   Whitfield, S., Fekadu, M., Olson, J.G., Rupprecht, C.E., Childs, J.E., 1998. Epidemiology

663   of human rabies in the United States, 1980 to 1996. Ann. Intern. Med. 128, 922–930.

664   doi:10.7326/0003-4819-128-11-199806010-00012

665 Oishi, S., Takano, R., Tamura, S., Tani, S., Iwaizumi, M., Hamaya, Y., Takagaki, K., Nagata, T.,
666   Seto, S., Horii, T., Osawa, S., Furuta, T., Miyajima, H., Sugimoto, K., 2016. M2
667   polarization of murine peritoneal macrophages induces regulatory cytokine production and
668   suppresses T-cell proliferation. Immunology 149, 320–328. doi:10.1111/imm.12647

669 Patton, J.B., Rowland, R.R., Yoo, D., Chang, K.O., 2009. Modulation of CD163 receptor
670   expression and replication of porcine reproductive and respiratory syndrome virus in
671   porcine macrophages. Virus Res. 140, 161–171. doi:10.1016/j.virusres.2008.12.002

672 Piazzon, M.C., Savelkoul, H.F.J., Pietretti, D., Wiegertjes, G.F., Forlenza, M., 2015. Carp Il10
673   Has Anti-Inflammatory Activities on Phagocytes, Promotes Proliferation of Memory T
674   Cells, and Regulates B Cell Differentiation and Antibody Secretion. J. Immunol. 194, 187–
675   199. doi:10.4049/jimmunol.1402093

676 Rahman, M.M., McFadden, G., 2011. Modulation of NF-κB signalling by microbial pathogens.
677   Nat. Rev. Microbiol. 9, 291–306. doi:10.1038/nrmicro2539

678 Ray, N.B., Ewalt, L.C., Lodmell, D.L., 1995. Rabies virus replication in primary murine bone
679   marrow macrophages and in human and murine macrophage-like cell lines: implications for
680   viral persistence. J. Virol. 69, 764–772.

681 Reed, L.J., Muench, H., 1938. A simple method of estimating fifty per cent endpoints. Am. J.
682   Hyg. 27, 546–558. doi:10.7723/antiochreview.72.3.0546

683 Saeed, R.W., Varma, S., Peng-Nemeroff, T., Sherry, B., Balakhaneh, D., Huston, J., Tracey,
684   K.J., Al-Abed, Y., Metz, C.N., 2005. Cholinergic stimulation blocks endothelial cell
685   activation and leukocyte recruitment during inflammation. J. Exp. Med. 201, 1113–1123.
686   doi:10.1084/jem.20040463

687 Sánchez-Torres, C., Gómez-Puertas, P., Gómez-Del-Moral, M., Alonso, F., Escribano, J.M.,
688   Ezquerra, A., Domínguez, J., 2003. Expression of porcine CD163 on
689   monocytes/macrophages correlates with permissiveness to African swine fever infection.
690   Arch. Virol. 148, 2307–2323. doi:10.1007/s00705-003-0188-4

691 Sang, Y., Miller, L.C., Blecha, F., 2015. Macrophage Polarization in Virus-Host Interactions. J.
692   Clin. Cell. Immunol. 06. doi:10.4172/2155-9899.1000311

693 Schnell, M.J., McGettigan, J.P., Wirblich, C., Papaneri, A., 2010. The cell biology of rabies
694   virus: Using stealth to reach the brain. Nat. Rev. Microbiol. 8, 51–61.

695 doi:10.1038/nrmicro2260

696 Scott, T.P., Nel, L.H., 2016. Subversion of the immune response by Rabies Virus. Viruses 8, 1–

697 26. doi:10.3390/v8080231

698 Shytle, R.D., Mori, T., Townsend, K., Vendrame, M., Sun, N., Zeng, J., Ehrhart, J., Silver, A.A.,

699 Sanberg, P.R., Tan, J., 2004. Cholinergic modulation of microglial activation by α7

700 nicotinic receptors. J. Neurochem. 89, 337–343. doi:10.1046/j.1471-4159.2004.02347.x

701 Stout, R.D., Jiang, C., Matta, B., Tietzel, I., Watkins, S.K., Suttles, J., 2005. Macrophages

702 Sequentially Change Their Functional Phenotype in Response to Changes in

703 Microenvironmental Influences. J. Immunol. 175, 342–349.

704 doi:10.4049/jimmunol.175.1.342

705 Sugano, N., Shimada, K., Ito, K., Murai, S., 1998. Nicotine inhibits the production of

706 inflammatory mediators in U937 cells through modulation of Nuclear Factor-kB activation.

707 Biochem. Biophys. Res. Commun. 252, 25–28. doi:10.1006/bbrc.1998.9599

708 Takahashi, H.K., Iwagaki, H., Hamano, R., Yoshino, T., Tanaka, N., Nishibori, M., 2006. Effect

709 of nicotine on IL-18-initiated immune response in human monocytes. J. Leukoc. Biol. 80,

710 1388–1394. doi:10.1189/jlb.0406236

711 Turner, G.S., Ballard, R., 1976. Interaction of mouse peritoneal macrophages with fixed rabies

712 virus in vivo and in vitro. J. Gen. Virol. 30, 223–231. doi:10.1099/0022-1317-30-2-223

713 van Westerloo, D.J., Giebelen, I.A., Florquin, S., Bruno, M.J., LaRosa, G.J., Ulloa, L., Tracey,

714 K.J., van der Poll, T., 2006. The Vagus Nerve and Nicotinic Receptors Modulate

715 Experimental Pancreatitis Severity in Mice. Gastroenterology 130, 1822–1830.

716 doi:10.1053/j.gastro.2006.02.022

717 Vidy, A., Chelbi-Alix, M., Blondel, D., 2005. Rabies Virus P Protein Interacts with STAT1 and

718 Inhibits Interferon Signal Transduction Pathways. J. Virol. 79, 14411–14420.

719 doi:10.1128/jvi.79.22.14411-14420.2005

720 Wang, Hong, Liao, H., Ochani, M., Justiniani, M., Lin, X., Yang, L., Al-Abed, Y., Wang,

721 Haichao, Metz, C., Miller, E.J., Tracey, K.J., Ulloa, L., 2004. Cholinergic agonists inhibit

722 HMGB1 release and improve survival in experimental sepsis. Nat. Med. 10, 1216–1221.

723 doi:10.1038/nm1124

724 Wang, Hong, Yu, M., Ochani, M., Amella, C.A., Tanovic, M., Susarla, S., Li, J.H., Wang,

725 Haichao, Yang, H., Ulloa, L., Al-Abed, Y., Czura, C.J., Tracey, K.J., 2003. Nicotinic

726   acetylcholine receptor α7 subunit is an essential regulator of inflammation. Nature 421,

727   384–388. doi:10.1038/nature01339

728   WHO, 2018. Expert consultation on rabies - Third report, World Health Organization - Technical

729   Report Series. Geneva.

730   Yamaoka, S., Ito, N., Ohka, S., Kaneda, S., Nakamura, H., Agari, T., Masatani, T., Nakagawa,

731   K., Okada, K., Okadera, K., Mitake, H., Fujii, T., Sugiyama, M., 2013. Involvement of the

732   rabies virus phosphoprotein gene in neuroinvasiveness. J. Virol. 87, 12327–12338.

733   doi:10.1128/JVI.02132-13

734   Yearley, J.H., Pearson, C., Shannon, R.P., Mansfield, K.G., 2007. Phenotypic variation in

735   myocardial macrophage populations suggests a role for macrophage activation in SIV-

736   associated cardiac disease. AIDS Res. Hum. Retroviruses 23, 515–524.

737   doi:10.1089/aid.2006.0211

738